Synthesis and Characterization of Advance PA6-*b*-PDMS Multiblock Copolymers

Yanyan Zhang, Hong Fan, Bo-Geng Li

State Key Laboratory of Chemical Engineering, Department of Chemical and Biological Engineering, Zhejiang University, Hangzhou 310027, China
Correspondence to: H. Fan (E-mail: hfan@zju.edu.cn)

ABSTRACT: Advance polyamide-6-*b*-polydimethylsiloxane (PA6-*b*-PDMS) multiblock copolymers were first synthesized via the polymerization in bulk. Binary carboxyl terminated PA6 was served as the hard segment and PDMS modified with hexamethylene diisocyanate (PDMS-NCO) was the soft segment. A series of PA6-*b*-PDMS copolymers based on different content and length of soft segments were obtained. Interestingly, Differential scanning calorimetry (DSC) studies revealed no obvious change in melting temperature after introducing PDMS segments to copolymers. The high melting temperatures indicated these copolymers possess potential applications in automotive industry that require high continuous use temperatures. DSC and transmission electron microscopy studies both demonstrated increasing the length and the content of the soft segment contributed to increasing of the degree of microphase separation. However, the improvement of thermal stability resulting from PDMS segments was also observed by thermo gravimetric analysis. © 2014 Wiley Periodicals, Inc. J. Appl. Polym. Sci. **2014**, *131*, 41114.

INTRODUCTION

Thermoplastic polyamide elastomers (TPEs)[1–4] are unique materials that display elasticity and thermal plastic nature. In some way, TPEs are more soft and flexible than plastics but can be reprocessed unlike the thermoset.

Block copolymers and blended materials are two important parts of TPEs. Representative blended TPEs are thermoplastic vulcanizates (TPVs)[5–10] obtained by blending thermoplastic and rubber. This method is so commercial that some of these materials have been applied by manufacturers. However, conventional TPVs based on polypropylene matrix and a crosslinked ethylene–propylene–diene terpolymer rubber phase were limited in use in conditions that require continuous use at temperatures exceeding 135°C. Therefore, Dow corning launched a class of unique materials called "Super-TPV" based on vulcanized silicone rubber particles dispersed in polyamide and other thermoplastic matrixes.[11–13] These materials show excellent thermal stability and chemical resistance. However, the high interfacial tension between extremely nonpolar silicone rubber and the polar polyamide leads to an unstable morphology with inferior mechanical properties.

Block copolymers also play an important role in TPEs. Block copolymers of A-B-A type or (A-B)$_n$ type belonging to TPEs have two incompatible segments, wherein one segment is crystalline under room temperature (hard segment) and, however, the other is amorphous (soft segment). Hard and soft domains cause microphase separation and help obtain the desired natures. The properties of TPEs depend on the types of two segments, their lengths, and mass ratios.

Polyamide has excellent thermal properties and chemical resistance, in particular acid and alkali resistance. Therefore, TPEs based on polyamide (TPEs) have been researched in recent years.[14,15] However, at first, the polyamide used was almost aramid,[16–18] which was expensive and difficult to be processed. So in recent years, aliphatic polyamides such as polyamide-12,[19–22] polyamide-6 (PA6),[23,24] and polyamide-4,6 have received high attention. Especially PA6 is one of the most important members of aliphatic polyamides with high melting temperature (T_m) and commercial advantages.

Polydimethylsiloxane (PDMS) shows many important properties, such as low glass transition temperature of about −128°C, which is about 50°C lower than polytetrahydrofuran.[25,26] Furthermore, PDMS has good weathering resistance, low surface tension, good biocompatibility, and so on. TPEs with PDMS used as the soft segment have been researched a lot, with the hard segment of polyester,[27–29] polyurethane,[30,31] and polyurea.[32–34] However, there has not any research about TPEs based on PA6 and PDMS yet.

Scheme 1. Synthesis and structure of PA6-*b*-PDMS multiblock copolymers.

Polyamide-6-*b*-polydimethylsiloxane (PA6-*b*-PDMS) multiblock copolymers exhibit phase separation due to the incompatibility between nonpolar PDMS segments and polar PA6 segments. PA6 segments can crystallize and form hard domains, which leads to excellent thermal stability of copolymers. Meanwhile, PDMS segments are amorphous and provide softness to copolymers. However, it is very difficult to get high molar weight by the polycondensation of binary carboxyl-terminated PA6 with hydroxypropyl-terminated PDMS, because of the extreme incompatibility between PA6 and PDMS segments. It has been discovered that some polar segments attached to the ends of PDMS prepolymers would perform as compatibilizer between the polar hard and the nonpolar PDMS segments.[35] In this research, a kind of TPEs based on PA6-*b*-PDMS multiblock copolymers was explored, and to promote the reactive ability between nonpolar PDMS and the polar PA6, the end functional group of PDMS was modified by hexamethylene diisocyanate (HDI). A class of TPEs based on PA6 and PDMS-NCO (PDMS modified by HDI) was synthesized. PA6 was the hard segment and PDMS-NCO was the soft segment. The aim of this study was to investigate the influence of soft lengths and mass ratios on the thermal properties and microphase separation of copolymers, which has not been researched before.

EXPERIMENTAL

Materials

PA6-*b*-PDMS multiblock copolymers were synthesized by the bulk polymerization of PA6, PDMS-NCO (PDMS modified by HDI), and HDI. PA6 was used as the hard segment, and PDMS-NCO was used as the soft segment, while HDI was used as a coupling reagent (see Scheme 1). ε-Caprolactam (CL) and adipic acid (AA) (99%, from Aladdin, Shanghai, China) were used as received. α,ω-Dihydroxypropyl-PDMS (99%, from Shanghai Silicone Chemical Company; number average molar mass $M_n = 1000$ g/mol and $M_n = 2000$ g/mol, respectively) was used as received. HDI (99%, from Aladdin, Shanghai, China) was used as received. Trifluoroacetic acid-d (CF₃COOD, $D > 99.5\%$, from J&K Scientific) and deuterium oxide (D₂O, $D > 99.9\%$, from J&K Scientific) were used as received.

Synthesis of PA6 via Hydrolytic Ring-Opening Polymerization

A 3.75-L stainless steel vessel, equipped with mechanical stirring and a nitrogen inlet and outlet, was charged with 2.0 kg CL, 157.5 g AA, and 60.0 g water. After purging with nitrogen for 15 min, the oil bath was heated to 250°C for 5 h. Then the pressure inside the vessel was decreased to normal pressure and transparent liquids in the vessel were poured out above 230°C. PA6 prepolymers turned into white solids at room temperature. Binary carboxyl terminated PA6 with theoretical M_n (number average molar mass) 2000 g/mol was obtained.

Preparation of Isocyanate-Terminated PDMS

Isocyanate-terminated PDMS (PDMS-NCO) was synthesized in a 250-mL round flask equipped with a condenser and a dropping funnel. After purging with N₂ for 15 min, 100 g α,ω-dihydroxypropyl-PDMS was heated to 100°C, and 2.1 equivalents of HDI was then added dropwise to PDMS. Under nitrogen protection

and constant stirring at 200 rpm, the mixture reacted up to 8 h. To ensure the reaction time, the mass ratio of isocyanate end groups (NCO) was titrated by di-*n*-butylamine. PDMS-1K-NCO and PDMS-2K-NCO were obtained, where 1K and 2K in the middle indicate the molecular weight of PDMS segments.

Synthesis of PA6-*b*-PDMS Multiblock Copolymers

The reactions were performed in a three-neck, round-bottom flask fitted with a mechanical stirrer, nitrogen inlet, and a dropping funnel. A two-step procedure was used during the synthesis. PA6 was added into the flask and heated to 235°C for melting. After PA6 melted completely, the calculated amounts of HDI was introduced into the dropping funnel and added into the reactor. After 15 min, the PDMS-NCO was added to the flask in the mass ratios (PDMS-NCO : PA6) 10 : 90, 20 : 80, and 30 : 70. This step was completed after 0.5 h and the products were taken out by forceps. The added amounts of HDI was determined by the mole ratios of n (COOH of PA6)/n(NCO of PDMS-NCO) to ensure the mole ratios were 1 : 1.

Characterization

Infrared (FT-IR) spectra were obtained by a Nicolet 5700 FT-IR spectrometer. Samples were compressed to thin film by a pressing machine under 220°C. The thickness of the film was about 0.5 mm. These films were used to collect the FT-IR spectra in the attenuated total reflection mode under room temperature.

Proton nuclear magnetic resonance (^{1}H NMR) experiments were performed on Bruker 500 MHz spectrometer. The ^{1}H NMR spectra were measured at 25°C using a mixture of CF$_3$COOD/D$_2$O ($v/v = 1/1$) as the solvent.

The gel permeation chromatography (GPC) was obtained on a Waters 1525/2414 instrument equipped with a refractive index detector at 25°C. The eluent was tetrahydrofuran (THF) at a flow rate of 1 mL/min and narrow molar weight distribution polystyrene samples were calibration standards.

Differential scanning calorimetry (DSC) of the products were obtained on a Q200 thermal analyses instrument, under nitrogen atmosphere with three cycles: the first scanning was heated to 250°C by 100°C/min and keep isothermal by 3 min to cancel previous thermal history; the second scanning was cooled to −150°C by 10°C/min; and the last scanning was heated to 250°C by 10°C/min. Thermo gravimetric analysis (TGA) was performed in a Perkin–Elmer TG thermal analyzer (Pyris 1 TGA) to determine the thermal stabilities of products. Experiments were performed under nitrogen atmosphere and the heating rate was 20°C/min from 0 to 600°C.

Transmission electron microscopy (TEM) data were obtained using a Tecnai T12 electron microscope. The samples were cut into slices (80–100 nm thickness) at −140°C. Microtomed sections were collected on copper grids and soaked in a 1.5% aqueous solution of phosphotungstic acid (PTA) for 60 min. PTA reacted with the amino group of polyamide and enhanced contrast in the TEM images. After dried under the infrared lamp, samples were observed by the microscope.

Titration of Carboxylic Acid End Groups of PA6. The concentration of the carboxyl groups (—COOH) of PA6 was deter-mined by titration with NaOH in ethanol solution (0.02 mol/L). Carboxyl-terminated PA6 (≈0.5 g) was weighed accurately into a 250-mL Erlenmeyer flask equiped with a magnetic stirbar. Benzyl alcohol (35 mL) was added to the Erlenmeyer flask, and the flask was heated to 135°C to dissolve PA6. After PA6 was dissolved completely, the flask was cooled down to room temperature along with five drops of ethanol solution of phe-nolphthalein (5 g/L) as the pH indicator. Then the mixture was titrated with NaOH in ethanol solution (0.02 mol/L) until a purple end point.

The GPC Analysis of PA6 by N-Trifluoroacetylation Modification. PA6 cannot be dissolved by the normal solvents of GPC. In this research, the PA6 was trifluoroacetylated for GPC analysis.[36] PA6 (≈50 mg) was weighed into a 100-mL flask, along with 2 mL trifluoroacetic anhydride (TFAA) and about 5 mL dichloromethane (DCM). The solution was placed under room temperature for 24 h. The rest TFAA and DCM was removed by reduced pressure distillation under 35°C. After the solvents were removed completely, THF was added into the flask to pre-pare a solution of 3 mg/mL for GPC analysis. The GPC analysis of PDMS-*b*-PA6 used the same procedure.

Titration of Isocyanate End Groups of PDMS-NCO. The concentrations of the NCO groups of PDMS-NCO were determined by titration with HCl aqueous solution (0.02 mol/L). PDMS-NCO (≈1.0 g) was weighed accurately into a 250 mL Erlenmeyer flask. Twenty milliliter *N*-butyl amine solution in toluene (0.2 mol/L) was added to the Erlenmeyer flask by suction pipet. After 30 min, five drops of ethanol solution of bromine methyl green (5 g/L) were added as the pH indicator. Then the mixture was titrated with HCl aqueous solution (0.02 mol/L) until a yellow end point.

RESULTS AND DISCUSSION

In this research, the synthesis and characterization of PA6-*b*-PDMS multiblock copolymers are presented. A binary carboxyl terminated PA6 was the hard segment, and PDMS-1K-NCO and PDMS-2K-NCO were the soft segments, respectively, while HDI was used as a coupling reagent. The influence of soft lengths and mass ratios on the thermal properties and morphology of copolymers were investigated.

Synthesis and Structure Analysis of Prepolymers PA6 and PDMS-NCO

Structure Analysis of the Hard Segment PA6. The hard segment PA6 was characterized by ^{1}H NMR spectroscopy. The ^{1}H NMR spectrum of PA6 is shown in Figure 1. The peaks of H (a) (see the molecular structure in Figure 1) at 2.62–2.65 ppm are related to CH$_2$ attached to carboxylic acid end groups. The peaks at 2.24–2.27 ppm are assigned to methylene groups CH$_2$ (b) and the peaks at 1.70–1.76 ppm correspond to methylene groups CH$_2$ (c) in the middle of AA group. Protons of methyl-ene groups CH$_2$ (d) from the repeated unites of PA6 appear at 3.34–3.36 ppm. The signals of methylene groups CH$_2$ (e) attached to amide groups appear at 3.24–3.27 ppm. Protons of methylene groups CH$_2$ (f), CH$_2$ (g), and CH$_2$ (h) in the central of PA6 repeated units appear at 1.58–1.62 ppm, 1.28 ppm, 1.48–1.54 ppm, respectively. The peaks at 2.38–2.43 are assigned
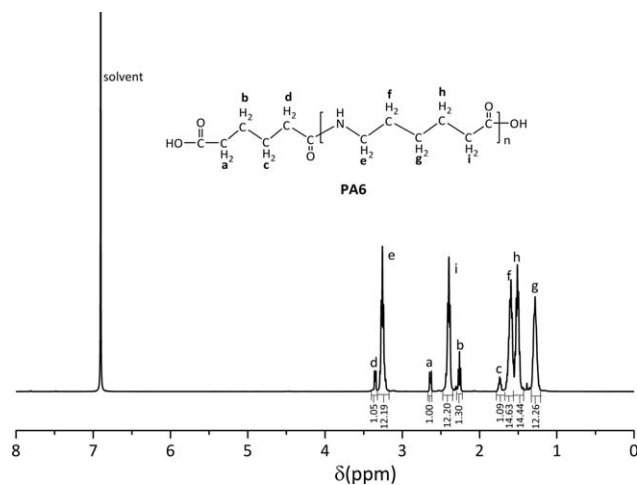
Figure 1. ^{1}H NMR spectroscopy of PA6.

to methylene groups CH_2 (i) attached to terminal carboxylic acid groups.

The number-average molecular weight M_n of PA6 (M_{nPA6}) was calculated from the ^{1}H NMR spectra, as the relative intensities of the methylene proton signals arising from the CH_2 (a) of the AA end groups and the methylene proton signals of the CH_2 (e) from the repeated unites of PA6.

$$M_{nPA6} = \frac{I[CH_2(e)]}{I[CH_2(a)]} \cdot M_{CL} + M_{AA} \quad (1)$$

where M_{CL} is the molecular weight of repeated unite of PA6, $M_{CL} = 113$ g/mol; M_{AA} is the molecular weight of the AA end group, $M_{AA} = 146$ g/mol. M_{nPA6} calculated by ^{1}H NMR spectroscopy was 1523 g/mol. Meanwhile, M_n of PA6 calculated by titration was 1980 g/mol.

The molecular weights of PA6 were also obtained by GPC and summarized in Table I. As the samples were modified by N-trifluoroacetylation before GPC analysis and the calibration standards were narrow molar weight distribution polystyrene samples, it is reasonable the GPC analysis values have larger differences with the actual molecular weights. However, determining the accurate contents of carboxyl end-groups is necessary for the next stage's reaction to ensure the mole ratios of n(COOH of PA6)/n(NCO) are 1 : 1. Compared with GPC anal-

ysis, the ^{1}H NMR spectra and titration results were more reliable. In this research, the amounts of the materials for the synthesis of PA6-b-PDMS were determined by titration.

Synthesis and Structure Analysis of the Soft Segment PDMS-NCO. The effects of the time on the formation of diisocyanate terminated PDMS (PDMS-NCO) are presented in Figure 2. To ensure hydroxyl groups of PDMS reacting with HDI as much as possible and avoid crosslinking, the contents of NCO groups in the reaction system were monitored by titration.

Figure 2 showed that PDMS reacted with HDI very fast under 100°C without catalyst. PDMS-1K showed a faster speed for its lower viscosity and higher content of reactive groups. The stable content of free NCO groups after 4 h indicated no obvious crosslinking, which is a good property for storage. However, to guarantee the sufficient reaction between HDI and PDMS, the time of the reaction was 8 h finally.

The FT-IR spectra of the samples PDMS-1K-NCO and PDMS-2K-NCO were shown in Figure 3. As shown in Figure 3, the absorption for the double bond of N=C=O (2273 cm^{-1}) attached to the soft segment PDMS-NCO is obvious. The peak at 1721 cm^{-1} is assigned to C=O contracting.

Structure Analysis of PA6-b-PDMS Copolymers
FT-IR and ^{1}H NMR Spectroscopy of PA6-b-PDMS Copolymers. The FT-IR spectroscopy of the copolymers 1c (PA6/PDMS-1K-NCO = 70 : 30) and 2c (PA6/PDMS-2K-NCO = 70 : 30) were presented in Figure 3. As shown in the FT-IR spectra, the absorption for the double bond of N=C=O (2273 cm^{-1}) attached to the soft segment PDMS-NCO disappeared. The peak at 3295 cm^{-1} is assigned to the stretching vibration of N—H, and the peak at 1632 cm^{-1} is assigned to the stretching vibration of C=O attached to the hard chain PA6, and the intensive bands at 1014 and 1085 cm^{-1} correspond to Si—O—Si in the copolymer's soft chain PDMS. The rest of the peaks at 2931 cm^{-1} and 2861 cm^{-1} are assigned to the presence of symmetric and asymmetric CH_2 groups.

The ^{1}H NMR spectroscopy and the molecular structure of the copolymer 1c (PA6/PDMS-1K-NCO = 70 : 30) is shown in Figure 4. Protons from the methylene groups CH_2 (1) appear at 2.65–2.67 ppm. The peaks at 2.26–2.29 ppm and the peaks at 1.77–1.79 ppm are assigned to methylene groups CH_2 (2)

Table I. GPC Analysis of the Synthesized PA6 and PA6-b-PDMS Copolymers

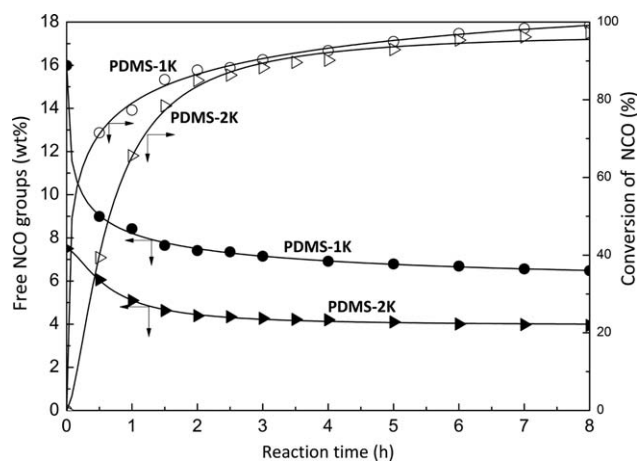| Sample	PA6/PDMS-NCO (w/w %)	M_n (kg/mol)	M_w (kg/mol)	PDI
PA6	100/0	5.30	8.20	1.55
The M_n of the used α,ω-dihydroxypropyl-PDMS was 1000 g/mol				
1a	90/10	10.7	42.3	3.95
1b	80/20	19.9	32.5	1.63
1c	70/30	16.2	40.9	2.52
The M_n of the used α,ω-dihydroxypropyl-PDMS was 2000 g/mol				
2a	90/10	23.9	46.4	1.94
2b	80/20	20.4	38.4	1.88
2c	70/30	22.3	41.3	1.85

Figure 2. Monitoring of the reaction of PDMS-1K and PDMS-2K with HDI by the dibutylamine back titration. [Color figure can be viewed in the online issue, which is available at wileyonlinelibrary.com.]
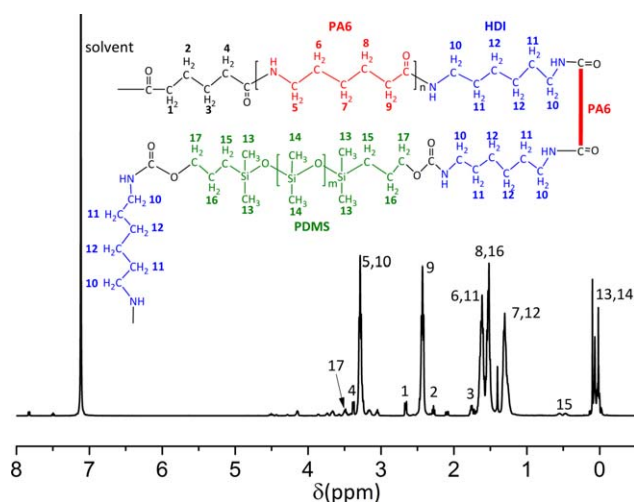

Figure 4. ^{1}H NMR spectroscopy of PA6-*b*-PDMS multiblock copolymer 1c (PA6/PDMS-1K-NCO = 70 : 30). [Color figure can be viewed in the online issue, which is available at wileyonlinelibrary.com.]

and CH$_2$ (3), respectively. The protons from methylene groups CH$_2$ (4) appear at 3.37–3.39 ppm. The peaks at 3.27–3.30, 1.72–1.76, 1.26–1.32, 1.50–1.56, and 2.42–2.45 ppm are related to methylene groups CH$_2$ (5), CH$_2$ (6), CH$_2$ (7), CH$_2$ (8), and CH$_2$ (9) in the PA6 segments, respectively. Protons from methylene groups CH$_2$ (10) which were assigned to HDI segments appear at 3.27–3.30 ppm with CH$_2$ (5). And protons from methylene groups CH$_2$ (11) appear at 1.72–1.76 ppm with CH$_2$ (6). The central methylene protons CH$_2$ (12) from HDI appear at 1.26–1.32 ppm with CH$_2$ (7). Methyl protons of the Si-CH$_3$ groups CH$_2$ (13, 14) appear at 0.02–0.10 ppm, and protons from methylene groups CH$_2$ (15), CH$_2$ (16), CH$_2$ (17) that related to PDMS segments appear at 0.43–0.49, 1.50–1.56, and 3.47–3.50 ppm, respectively.

GPC Analysis of PA6-*b*-PDMS Copolymers. The molecular weights obtained from GPC for synthesized PA6-*b*-PDMS are summarized in Table I. The M_w values of PA6-*b*-PDMS range

from 32.5 to 46.4 kg mol^{-1}, with a polydispersity index ranging from 1.63 to 3.95. The increase in the molecular weights of copolymers compared with PA6 proved the hard segments PA6 reacted with the soft segments PDMS-NCO successfully, especially as presented in Figure 5. Although GPC analysis results had obvious difference with actual molecular weights, it is still useful to compare the GPC curves of PA6 segments with those of PA6-*b*-PDMS copolymers. As presented in Figure 5, the log M_w of PA6-*b*-PDMS 1c is higher than that of PA6, in addition, only one peak can be observed, and this demonstrates that all PA6 segments were linked to the PDMS segments.

DSC Analysis of PA6-*b*-PDMS Copolymers

The DSC analysis of PA6-*b*-PDMS copolymers is presented in Figure 6 and Table II. It is very apparent the copolymers have two glass transition temperature (T_g), one for PDMS segments and one for PA6 segments, and the DSC thermograms of the copolymers show one clear endotherm attributed to the melting
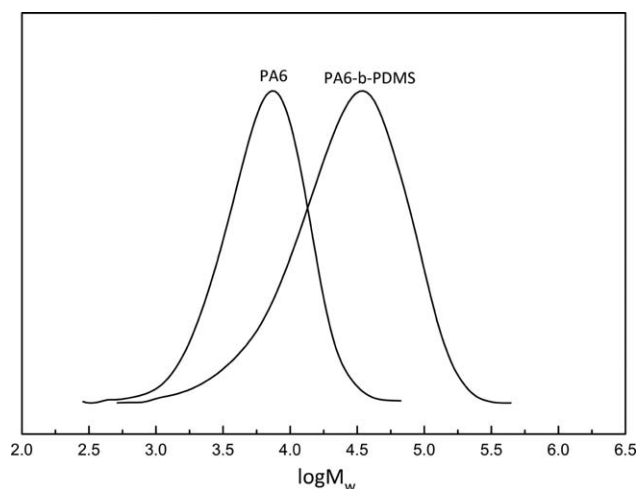

Figure 3. FT-IR spectra of PA6, PDMS-1K-NCO, 1c (PA6/PDMS-1K-NCO = 70 : 30), PDMS-2K-NCO, 2c (PA6/PDMS-2K-NCO = 70 : 30). [Color figure can be viewed in the online issue, which is available at wileyonlinelibrary.com.]

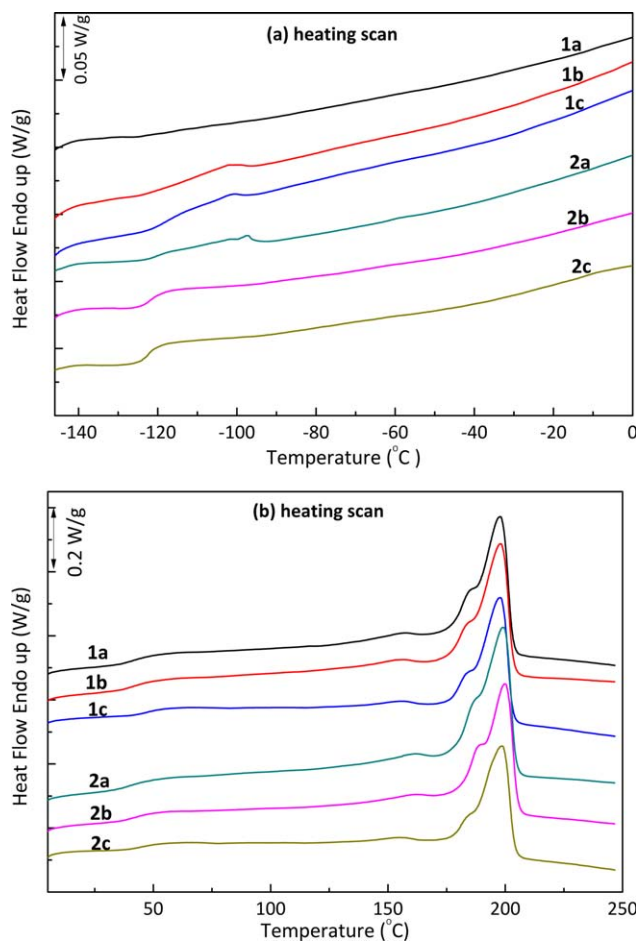**Figure 5.** GPC curves of PA6 and PA6-*b*-PDMS copolymer 1c.

Figure 6. DSC thermograms of synthesized PA6-*b*-PDMS multiblock copolymers: (a) second heating run from −150°C to 0°C, (b) second heating run from 0°C to 250°C. [Color figure can be viewed in the online issue, which is available at wileyonlinelibrary.com.]

temperature (T_m) of the hard segments PA6. There is no obvious change in T_m resulting from the same length of the PA6 chains. The melting temperatures of the PA6 segments in the PA6-*b*-PDMS copolymers were 198–200°C. Introducing of HDI connected two PA6 segments together and formed new amide groups. The interaction of hydrogen bounding between the PA6 segments was enhanced. The T_m of copolymers is much higher than conventional TPEs, such as thermoplastic polyurethanes and olefinic TPVs. This result shows that these copolymers possess potential applications in industry such as automotive body plugs, seals, and underhood hoses.

From Table II, the decrease in enthalpy of copolymers can be observed with the increasing content of soft segments. Copolymers exhibit phase separation due the incompatibility between PA6 segments and PDMS segments. PA6 segments are crystalline, and PDMS segments are amorphous. So with the decreasing content of PA6 segments, the area of crystalline regions reduced and the enthalpy of copolymers decreased.

Meanwhile, apparent changes can be observed in the T_g of PDMS and PA6 segments. The $T_{g\text{-PDMS}}$ attribute to the T_g of PDMS chains and $T_{g\text{-PA6}}$ due to PA6 chains. Two clear T_g indi-

cate that PDMS soft segments in the PA6-*b*-PDMS copolymers mostly are not contaminated by PA6 hard segments and display a high degree of phase separation between the hard segment and the soft segment. The degree of phase separation of PA6-*b*-PDMS multiblock copolymers is higher than that of polyamide–polyether multiblock copolymers. This is because PDMS segments are extremely hydrophobic, but PA6 segments are extremely hydrophilic. There is not any hydrogen bonding between PA6 and PDMS segments. The higher incompatibility between the two segments leads to a higher degree of phase separation.

The $T_{g\text{-PDMS}}$ of 1a is not discernible in the DSC thermogram. That is the cause of lowest PDMS content and the few PDMS segments dispersed in the hard segments, so the motion of the soft segment is highly limited. The degree of phase separation between the hard and soft phase of PA6-*b*-PDMS copolymers can be determined by the variation in T_g and the breadth of the soft segment glass transition temperature (ΔB). The glass transition temperature $T_{g\text{-PDMS}}$ of copolymers were higher than those of pure PDMS-1K ($T_g = -118°C$) and PDMS-2K ($T_g = -122°C$) when the soft segments mass ratio was less than 20 wt %. This can be explained by a small amount of soft segments mixing within the hard domains. The increase in the ΔB values imply decreasing degree of phase separation between the soft phase and the hard phase.[31,37] Table II shows that the ΔB values of PA6-*b*-PDMS copolymer were 3–13°C. The samples 1b and 1c have very high ΔB values due to the shorter length of the soft segments, implying the formation of a mixed phase between the soft and the PA6 hard segments. Notably, the ΔB value of sample 2c is minimal attribute to the longer length and highest content of the soft segments. Accordingly, the increasing degree of phase separation for PA6-*b*-PDMS copolymers possibly results from the increasing content and longer length of soft segments.

Morphological Characteristics of PA6-*b*-PDMS
The microstructures of PA6-*b*-PDMS Multiblock copolymers were examined by transmission electron microscopy (TEM). The representative images are shown in Figure 7. Samples were stained by aqueous solution of PTA to enhance contrast in the TEM images. The light and dark microdomains are associated with PDMS and PA6 domains, respectively. These images indicate highly incompatible between extremely nonpolar PDMS segments and the polar PA6 segments. This immiscibility leads to PDMS segments curling upto huddle together in PA6 domains, and form obvious phase separation.

As shown in Figure 7, increasing the content of the PDMS segments contributes to larger degree of phase separation, which confirms the same trend of DSC results. Compared with the copolymers 1a, 1b, and 1c, the copolymers 2a, 2b, and 2c have neater PDMS domains. Longer length of PDMS segments makes it more difficult to blend PA6 segments in the soft domains. Consequently, increasing content and longer length of soft segments results in the increasing degree of phase separation.

Thermal Stability Analysis of PA6-*b*-PDMS Copolymers
The thermal degradation behavior of PA6-*b*-PDMS copolymers was measured by TG in nitrogen and present in Figure 8. The TG curves show the similar trend of all the PA6-*b*-PDMS

Table II. DSC Analysis of the Synthesized PA6-b-PDMS Copolymers

Sample	$T_{g\text{-PDMS}}$ (°C)[a]	ΔB_{PDMS} (°C)[b]	$T_{g\text{-PA6}}$ (°C)[c]	$T_{c\text{-PA6}}$ (°C)[d]	ΔH_c (J/g)[e]	$T_{m\text{-PA6}}$ (°C)[f]	ΔH_m (J/g)[g]	$T_{d,5}$ (°C)[h]	$T_{d,\max}$ (°C)[i]
PA6-2K			–	163.7	52.9	198.5	48.0	289	384
PDMS-1K	−118	6						232	446
PDMS-2K	−122	4						285	456
1a	–	–	41.4	154.8	41.8	198.1	37.5	300	462
1b	−110	13	40.8	153.8	39.2	198.3	35.5	329	460
1c	−118	9	46.5	154.1	35.3	198.1	31.6	339	460
2a	−120	9	39.7	159.8	46.9	199.5	39.8	347	462
2b	−122	4	43.6	158.4	37.5	200.2	32.5	344	462
2c	−122	3	44.5	153.1	31.9	198.8	28.9	368	462

$\Delta B_{\text{PDMS}} = |T_2 - T_1|$, where T_1 is the temperature at which the glass transition of PDMS segments starts; T_2 is the temperature at which the glass transition of PDMS segments is over.
[a] Glass transition temperature of PDMS segments.
[b] The breadth of the soft segment glass transition temperature.
[c] Glass transition temperature of PA6 segments.
[d] Crystallization temperature of PA6 segments.
[e] The enthalpy of crystallization of PA6 segments.
[f] Melting temperature of PA6 segments.
[g] The enthalpy of melting of PA6 segments.
[h] Decomposition temperature of 5 wt % weight loss.
[i] Decomposition temperature of maximum weight loss speed.

samples. The decomposition temperatures of 5 wt % weight loss are observed between 300 and 368°C, and close temperature of maximum decomposition speed occur around 460°C. The results of the TG measurements are summarized in Table II.

Although the temperature at which the decomposition speed is fastest is almost constant regardless of the soft segment content, the temperature of 5 wt % weight loss increase with increasing soft segments content. The sample 1a with minimum soft segments content (10 wt %) and shorter length of PDMS segments degrade for 5 wt % at 300°C, while the sample 2c with maximum soft segments content (30 wt %) and longer length of PDMS segments is at 360°C. This can be explained by the higher thermal stability of PDMS segments in comparison with PA6 segments, and the increasing of the content of the PDMS content can enhance the copolymers' thermal stability.
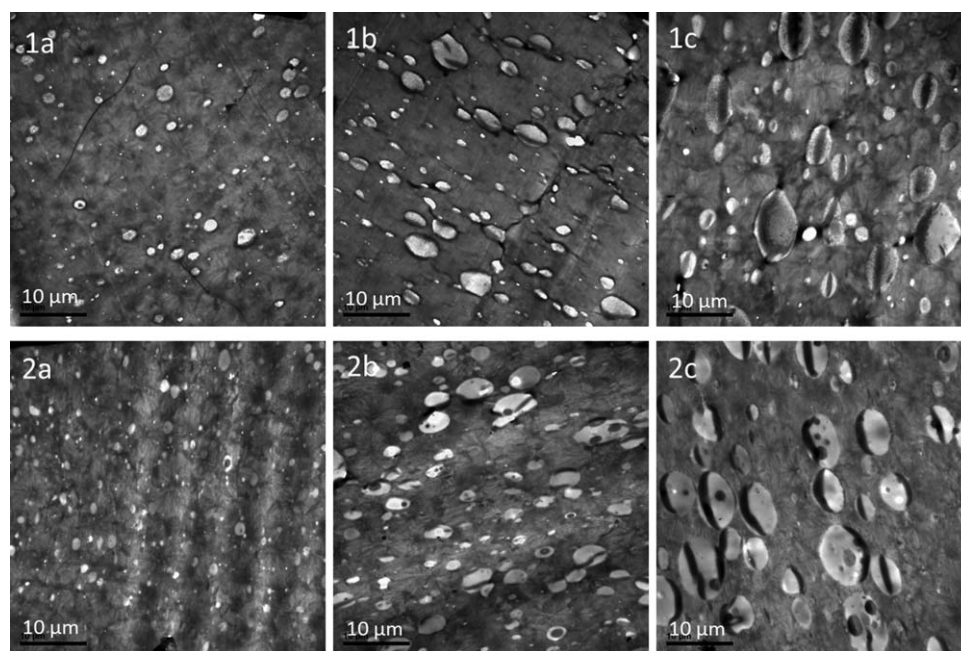

Figure 7. TEM images of PA6-b-PDMS copolymers (Samples were stained by aqueous solution of PTA. The light and dark microdomains are associated with PDMS and PA6 domains, respectively). [Color figure can be viewed in the online issue, which is available at wileyonlinelibrary.com.]
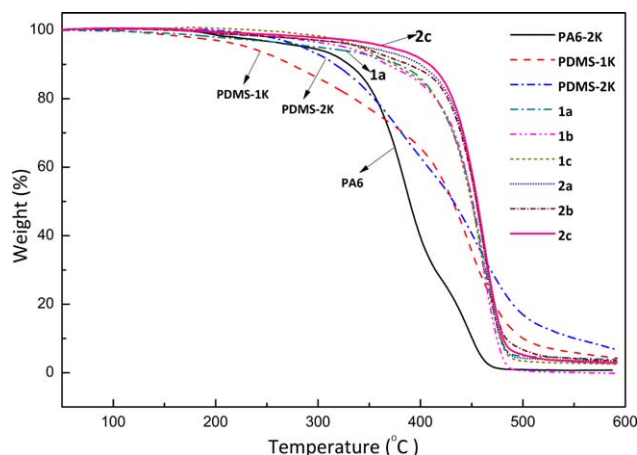
Figure 8. TG curves of the synthesized PA6-*b*-PDMS copolymers. [Color figure can be viewed in the online issue, which is available at wileyonlinelibrary.com.]

CONCLUSIONS

Advance PA6-*b*-PDMS multiblock copolymers were firstly synthesized in this research. Binary carboxyl terminated PA6 was served as the hard segments, and PDMS-NCO was used as the soft segment. DSC analysis results showed the copolymers had one T_m contributing to the hard segments PA6 and two T_g resulting from PDMS segments and PA6 segments, respectively. The melting temperatures of PA6-*b*-PDMS copolymers were 198–200°C. Meanwhile, introducing PDMS segments contributed to a very low T_g (-118 to -122°C). DSC and TEM analysis also showed that increasing the length and the content of the soft segment contribute to increasing of the degree of the microphase separation, while the increasing of the content of the PDMS content can enhance the thermal stability of copolymers. Actually, it was shown that the PDMS segments were very incompatible with PA6 segments, so introducing longer polar segments attached to the ends of PDMS prepolymers between PA6 and PDMS segments are encouraging.

ACKNOWLEDGMENTS

REFERENCES

1. Drobny, J. G. In Handbook of Thermoplastic Elastomers, Chapter 1; Elsevier: New York, **2007**; p. 2.

2. Markarian, J. *Plastics Additives Compound.* **2008**, *10*, 38.

3. George, J.; Varughese, K. T.; Thomas, S. *Polymer* **2000**, *41*, 1507.

4. Cespedes, R.; Gamez, J.; Velazquez, M.; Belmontes, F. A.; de Leon, R.; Fernandez, O.; Orta, C.; Hernandez, E. H. *J. Appl. Polym. Sci.* **2014**, *131*, 39901.

5. Drobny, J. G. In Handbook of Thermoplastic Elastomers, Chapter 1; Elsevier: New York, **2007**; p 4.

6. Holden, G.; Kricheldorf, H. R.; Quirk, R. P. In Thermoplastic Elastomers, Chapter 9; Hanser: Munich, **1996**; p 217.

7. Kalkornsurapranee, E.; Nakason, C.; Kummerlowe, C.; Vennemann, N. *J. Appl. Polym. Sci.* **2013**, *128*, 2358.

8. Zhu, Y. L.; Zhang, X. H.; Song, Z. H.; Qi, G. C.; Wang, X.; Li, B. H.; Wang, H. S.; Qiao, J. L. *J. Appl. Polym. Sci.* **2013**, *127*, 3885.

9. Wu, H. G.; Ning, N. Y.; Zhang, L. Q.; Tian, H. C.; Wu, Y. P.; Tian, M. *J. Polym. Res.* **2013**, *20*, 266.

10. Wu, H. G.; Tian, M.; Zhang, L. Q.; Tian, H. C.; Wu, Y. P.; Ning, N. Y. *Soft Matter* **2014**, *10*, 1816.

11. Gornowicz, G. A.; Lupton, K. E.; Romenesko, D. J.; Struble, K.; Zhang, H. Dow Corning Corp.1999; WO1999045072 A1. Thermoplastic silicone elastomers.

12. Brewer, C. M.; Chorvath, I.; Lee, M. K.; Lee, Y.; Li, D.; Nakanishi, K.; Oldinski, R. L.; Petroff, L. J.; Rabe, R. L.; Romenesko, D. J. Dow Corning; Dow Corning Asia Ltd. 2002; WO2002008335 A2. Thermoplastic silicone elastomers from compatibilized polyamide resins.

13. Blackwood, W.; Nguyen, K.; Rabe, R.; Ryan, K. Dow Corning Corp. 2008; EP1569985 B1. Siloxane based amide modified nylons.

14. Buckwalter, D. J.; Inglefield, D. L.; Enokida, J. S.; Hudson, A. G.; Moore, R. B.; Long, T. E. *Macromol. Chem. Phys.* **2013**, *214*, 2073.

15. Kucera, L. R.; Brei, M. R.; Storey, R. F. *Polymer* **2013**, *54*, 3796.

16. Kang, E. C.; Kaneko, T.; Shiino, D.; Akashi, M. *J. Polym. Sci. Part A: Polym. Chem.* **2003**, *41*, 841.

17. Boulares, A.; Tessier, M.; Marechal, E. *Polymer* **2000**, *41*, 3561.

18. Otsuki, T.; KAKIMOTO, M.; Imai, Y. *Polym. J.* **1992**, *24*, 347.

19. Kozlowska, A.; Ukielski, R. *Eur. Polym. J.* **2004**, *40*, 2767.

20. Mani, S.; Cassagnau, P.; Bousmina, M.; Chaumont, P. *Macromol. Mater. Eng.* **2011**, *296*, 909.

21. Ukielski, R. *Polymer* **2000**, *41*, 1893.

22. Sheth, J. P.; Xu, J.; Wilkes, G. L. *Polymer* **2003**, *44*, 743.

23. Kucera, L. R.; Brei, M. R.; Storey, R. F. *Polymer* **2013**, *54*, 3796.

24. Yi, C.; Peng, Z.; Wang, H.; Li, M.; Wang, C. *Polym. Int.* **2011**, *60*, 1728.

25. Mark, J. E. In Polymer Data Handbook; Oxford University Press: New York, **2009**; p 849.

26. Petr, M.; Katzman, B. A.; DiNatale, W.; Hammond, P. T. *Macromolecules* **2013**, *46*, 2823.

27. Antić, V. V.; Govedarica, M. N.; Djonlagic, J. *Polym. Int.* **2004**, *53*, 1786.

28. Antić, V. V.; Pergal, M. V.; Govedarica, M. N.; Antić, M. P.; Djonlagić, J. *Polym. Int.* **2010**, *59*, 796.

29. Antić, V. V.; Govedarica, M. N.; Djonlagic, J. *Polym. Int.* **2003**, *52*, 1188.

30. Pergal, M. V.; Antić, V. V.; Govedarica, M. N.; Goäevac, D.; Ostojić, S.; Djonlagić, J. *J. Appl. Polym. Sci.* **2011**, *122*, 2715.

31. Tsi, H.; Chen, C.; Tsen, W.; Shu, Y.; Chuang, F. *Polym. Test.* **2011**, *30*, 50.

32. Sheth, J. P.; Aneja, A.; Wilkes, G. L.; Yilgor, E.; Atilla, G. E.; Yilgor, I.; Beyer, F. L. *Polymer* **2004**, *45*, 6919.

33. Sheth, J. P.; Yilgor, E.; Erenturk, B.; Ozhalici, H.; Yilgor, I.; Wilkes, G. L., *Polymer* **2005**, *46*, 8185.

34. Kinning, D. J. *J. Adhesion* **2001**, *75*, 1.

35. Vučković, M. V.; Antić, V. V.; Govedarica, M. N.; Djonlagić, J. *J. Appl. Polym. Sci.* **2010**, *115*, 3205.

36. Jeon, H. K.; Feist, B. J.; Koh, S. B.; Chang, K.; Macosko, C. W.; Dion, R. P. *Polymer* **2004**, *45*, 197.

37. Martin, D. J.; Poole Warren, L. A.; Gunatillake, P. A.; McCarthy, S. J.; Meijs, G. F.; Schindhelm, K. *Biomaterials* **2000**, *21*, 1021.